Solvent Effects on the Thioamide Rotational Barrier: An Experimental and Theoretical Study

Kenneth B. Wiberg* and Daniel J. Rush

Contribution from the Department of Chemistry, Yale University, New Haven, Connecticut 06520-8107

Received October 4, 2000. Revised Manuscript Received December 27, 2000

Abstract: The solvent effect on the C−N rotational barriers of *N*,*N*-dimethylthioformamide (DMTF) and *N*,*N*-dimethylthioacetamide (DMTA) has been investigated using ab initio theory and NMR spectroscopy. Selective inversion recovery NMR experiments were used to measure rotational barriers in a series of solvents. These data are compared to ab initio results at the G2(MP2) theoretical level. The latter are corrected for large amplitude vibrational motions to give differences in free energy. The calculated gas phase barriers are in very good agreement with the experimental values. Solvation effects were calculated using reaction field theory. This approach has been found to give barriers that are in good agreement with experiment for many aprotic, nonaromatic solvents that do not engage in specific interactions with the solute molecules. The calculated solution-phase barriers for the thioamides using the above solvents are also in good agreement with the observed barriers. The solvent effect on the thioamide rotational barrier is larger than that for the amides because the thioamides have a larger ground-state dipole moment, and there is a larger change in dipole moment with increasing solvent polarity. The transition-state dipole moments for the amides and thioamides are relatively similar. The origin of the C−N rotational barrier and its relation to the concept of amide "resonance" is examined.

1. Introduction

The properties of amides have received much attention because of their relationship to peptide conformations. An important aspect of amides is their preference for a near-planar arrangement of the amide group, and thus an understanding of structural and solvent effects on the barrier to C−N bond rotation is of some importance. This barrier has been investigated both experimentally and theoretically. We have determined the activation barriers for rotation of both *N*,*N*-dimethylformamide (DMF) and *N*,*N*-dimethylacetamide (DMA) in a variety of solvents, and we have correlated these energies with those calculated via a reaction field model.[1] G2(MP2)[2] calculations reproduced the observed gas-phase barriers,[3] and the reaction field model reproduced the solvent effects found in many aprotic polar solvents.[1]

We have also carried out theoretical studies of the barrier in thioamides and were able to reproduce the observed increase in rotational barrier on going from amides to thioamides.[4] An examination of the change in electron density at O or S that results from the rotation found that, whereas there was only a small degree of charge transfer from nitrogen to oxygen in the amides, there was a considerably larger charge transfer in the thioamides. In both cases, there was a shift in the σ-electron density in a direction opposite to that of the shift in π-electron density.

We have continued this study by measuring the effect of solvents on the C−N rotational barriers in *N*,*N*-dimethylthioformamide (DMTF) and *N*,*N*-dimethylthioacetamide (DMTA). True, et al. have recently measured the gas-phase rotational barriers for these compounds,[5] thus allowing a direct comparison between the gas phase and solutions. We have calculated the gas-phase barrier via the G2(MP2) model,[2] and we have estimated the solvent effect on the barrier using the SCI-PCM reaction field model.[6] These data will allow a more detailed analysis of the rotational barriers in amides. They also provide an additional example in which the gas-phase and solution energies of reaction may be compared.[1,6,7]

2. Experimental Determination of the Barriers in Thioamides

The C−N rotational barriers of DMTF and DMTA were measured in the same fashion as for our study of DMF and DMA.[1] Here, the NMR selective inversion recovery method was employed,[8−9] examining the methyl protons at 300 MHz as described in the Experimental Section. We have determined the rotational barriers in a series of solvents chosen to represent a wide range of polarity and to include both protic and aprotic examples. Table 1 contains the experimental data for DMTF and DMTA.

The methyl NMR signals for DMTA could be resolved in most cases, and measurements were made at 50.0° and 80.0

(1) Wiberg, K. B.; Rablen, P. R.; Rush, D. J.; Keith, T. A. *J. Am. Chem. Soc.* **1995**, *117*, 4261.
(2) Curtiss, L. A.; Raghavachari, K.; Pople, J. A. *J. Chem. Phys.* **1993**, *98*, 1293.
(3) Ross, B. D.; True, N. S. *J. Am. Chem. Soc.* **1984**, *106*, 2451. Ross, B. D.; True, N. S.; Matson, G. B. *J. Phys. Chem.* **1984**, *88*, 2675. LeMaster, C. B.; True, N. S. *J. Phys. Chem.* **1989**, *93*, 1307.
(4) Wiberg, K. B.; Rablen, P. R. *J. Am. Chem. Soc.* **1995**, *117*, 2201.
(5) Neugebauer C. S. M.; Taha, A. N.; True, N. S.; LeMaster, C. B. *J. Phys. Chem.* **1997**, *101*, 4699.
(6) Foresman, J. B.; Keith, T. A.; Wiberg, K. B.; Snoonian, J.; Frisch, M. J. *J. Phys. Chem.* **1996**, *100*, 16098.
(7) Wiberg, K. B.; Keith, T. A.; Frisch, M. J.; Murcko, M. *J. Phys. Chem.* **1995**, *99*, 9072.
(8) Dahlquist, F. W.; Longmuir, K. J.; DuVernet, R. B. *J. Magn. Reson.* **1975**, *17*, 406. Mann, B. E. *J. Magn. Reson.* **1976**, *21*, 17. Alger, J. R.; Prestegard, J. H. *J. Magn. Reson.* **1977**, *27*, 137. Led, J. J.; Gesmar, H. *J. Magn. Reson.* **1982**, *49*, 444. Gesmar, H.; Led, J. J. *J. Magn. Reson.* **1986**, *68*, 95. Grassi, M.; Mann, B. E.; Pickup, B. T.; Spencer, C. M. *J. Magn. Reson.* **1986**, *69*, 92. Engler, R. E.; Johnston, E. R.; Wade, C. G. *J. Magn. Res.* **1988**, *77*, 377.
(9) Perrin, C. L.; Thoburn, J. D.; Kresge, A. J. *J. Am. Chem. Soc.* **1992**, *114*, 8800.

10.1021/ja003586y CCC: $20.00
Published on Web 02/08/2001

Table 1. Solvent Effect on the Rotational Barriers for *N*,*N*-Dimethylthioformamide (DMTF) and *N*,*N*-Dimethylthioacetamide (DMTA) at 80 °C

medium	ϵ^a	DMTF	DMTA
gas phase	1.00	22.0[b]	17.7[b]
cyclohexane	1.93	23.5	19.6
carbon tetrachloride	2.09	23.6	20.3
benzene	2.18	24.8	21.3
toulene	2.21	24.6	21.0
n-butyl ether	2.9	*b*	20.1
chloroform	4.8	*b*	21.6
dichloromethane	9.0	*b*	(21.9)[c]
acetone	18.3	*b*	21.7
acetonitrile	32.7	25.4	22.2
water	61.0	(26.8)[d]	23.4

[a] The 80 °C dielectric constants were derived from the data in "Landolt-Bornstein," Vol. II, part 6, p 665ff, Springer-Verlag, Berlin, 1959. With di-*n*-butyl ether, the dielectric constant was assumed to be inversely proportional to the volume, which is generally the case. [b] Reference 5. [c] The two methyl signals could not be resolved in these solvents. [d] Based on rate constant at 50 °C. [e] Based on rate constant at 120 °C.

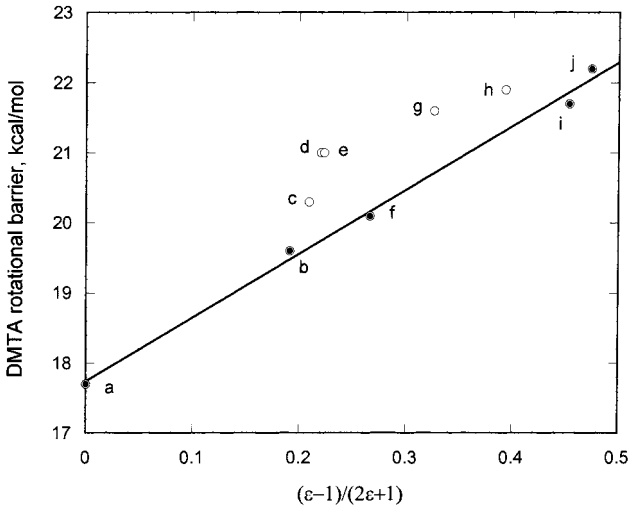

Figure 1. Correlation of the experimental C−N rotational barriers for DMTA with the Onsager function, $(\epsilon - 1)/(2\epsilon + 1)$. The line is drawn for the closed circles. The media are: (a) gas phase, (b) cyclohexane, (c) carbon tetrachloride, (d) benzene, (e) toluene, (f) di-*n*-butyl ether, (g) chloroform, (h) methylene chloride, (i) acetone, (j) acetonitrile.

°C. The $\Delta G^{\ddagger}$ increased slightly with temperature, suggesting a small negative entropy of activation. This also was found in the gas-phase studies.[5] Since the difference between the values at the two temperatures that we used was on the order of the estimated uncertainty in $\Delta G^{\ddagger}$, no meaningful $\Delta S^{\ddagger}$ values could be derived from the data. The 80.0 °C data are given in Table 1. With DMTF the NMR signals could not be resolved in some solvents, and therefore the data for this compound are more limited.

We have found in previous studies that the free energy changes caused by aprotic solvents such as cyclohexane, di-*n*-butyl ether, acetone, and acetonitrile are well correlated with the Onsager function,[10] $(\epsilon - 1)/(2\epsilon + 1)$ where ϵ is the dielectric constant of the solvent. A correlation of this type for DMTA is shown in Figure 1 where the line is drawn for the above solvents. There is also a group of aprotic solvents that usually give an enhanced solvent effect, and they include the aromatic solvents such as benzene and toluene, as well as the halogenated solvents such as carbon tetrachloride. These solvents also give an enhanced effect in the present case. As noted by Newton,[11] they have a low dielectric constant because they do not have a permanent dipole moment, but some also have a large quadrupole moment that can help stabilize polar solutes, and in addition, others such as carbon tetrachloride have high polarizability that can also stabilize polar solutes. This has not, as yet, been incorporated into the reaction field model.

With structurally similar compounds one might expect the solvent effects to be related. A plot of the DMF $\Delta G^{\ddagger}$ values against the corresponding DMA $\Delta G^{\ddagger}$ values was found to be linear with a slope of 0.55.[1] The smaller effect of solvents on DMF as compared to that on DMA is in accord with the difference in preferred rotational transition states for the two amides. The solvent dependence of the DMA barriers is governed by a large dipole moment difference between the ground state (GS) and the transition state having the lone pair anti to the carbonyl oxygen (TS1). In contrast, the solvent dependence of the DMF barriers is governed by a relatively small dipole moment difference between the GS and the transition state having the lone pair syn to the carbonyl oxygen (TS2). As a result, the solvent effect for DMA should be significantly stronger than that for DMF, as is observed in the experimental data. The change from TS2 for DMF to TS1 for DMA is a result of the steric interaction between the acetyl methyl group and the methyl groups at N in TS2 for DMA.[1]

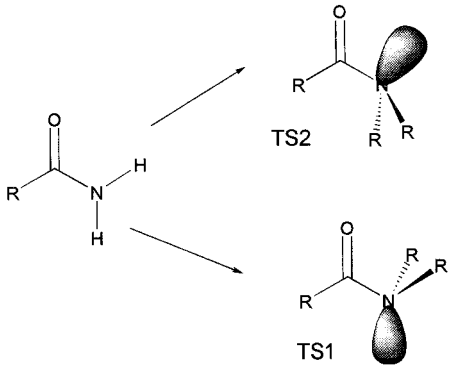

A similar effect is observed for the thioamides. A plot of $\Delta G^{\ddagger}$ values for DMTF against the corresponding DMTA barriers has some scatter, and the slope is 0.75 as shown in Figure 2. The larger slope of the line in Figure 2 indicates that the differences in solvent effect are less pronounced for the above thioamides than for the corresponding amides. This is not surprising since the thioamide TS2 has a lower dipole moment than the ground state, where in the amide system they are nearly equal. Thus, the thioamide TS2 experiences more of a solvent effect than the amide TS2, and this leads to a reduction in the difference between the two pathways.

Given the structural similarities of amides and thioamides, we might expect solvents to have similar effects on the rotational barrier for an amide and its corresponding thioamide. Figure 3 shows a plot of the observed C−N rotational barriers in a variety of solvents for DMTA against those of DMA. The relationship is approximately linear with a slope of 1.7. This larger slope clearly reflects a greater solvent effect on the thioamide than on the amide. The calculations described below find a considerably larger ground-state dipole moment for DMTA than for

(10) Onsager, L. *J. Am. Chem. Soc*. **1936**, *58*, 1486.

(11) Perng, B. C.; Newton, M. D.; Raineri, F. F.: *J. Chem. Phys.* **1996**, *104*, 7153.

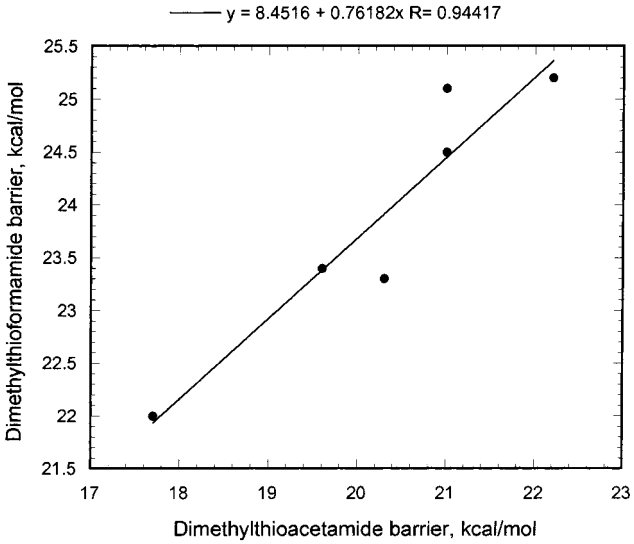

Figure 2. Correlation of the DMTF rotational barrier with the DMTA barrier.

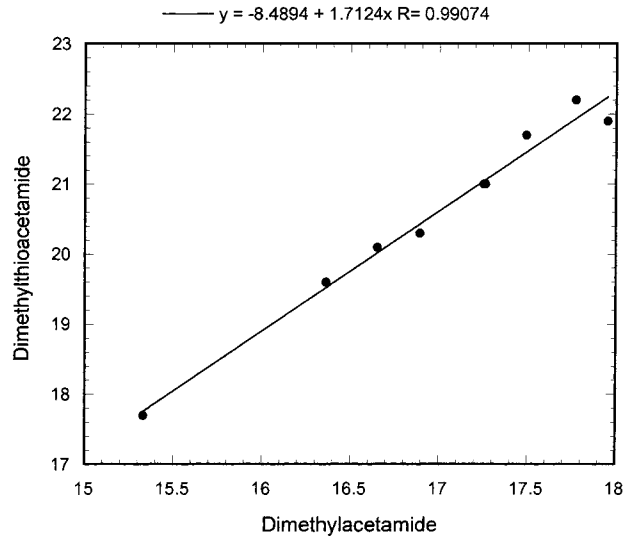

Figure 3. Correlation of the DMTA C−N rotational barrier with the DMA rotational barrier.

DMA (5.83 vs 4.37D), whereas the TS dipole moments are essentially the same (2.45 vs 2.33 D).

The specific interactions which cause some solvents to deviate from linearity in Figure 1 have very similar effects on both amide and thioamide rotational barriers. The consistent pattern of data points in Figure 3 reinforces the conclusion that these effects are based on intrinsic properties of the solvents.

3. Gas-Phase C−N Rotational barriers

To make a detailed comparison of the calculated and observed rotational barriers, it is first necessary to be able to reproduce the gas-phase values. The experimental values at 80 °C are 17.7 and 22.0 kcal/mol for DMTA and DMTF, respectively, measured using gas-phase NMR spectroscopy by True and coworkers[5] The smaller barrier for DMTA is probably due to a steric repulsion between the acetyl methyl group and the nearby *N*-methyl group, as was found with DMA.[1]

The G2(MP2) model chemistry has been found to reproduce the gas-phase barriers for DMF and DMA when the terms in the correction to the temperature used in the experiments were separately calculated for the methyl rotational modes and the nitrogen inversion vibration.[1] The usual harmonic oscillator approximation is not appropriate for these large amplitude mode. The above procedure has now been used to estimate the barriers for DMTF and DMTA at 353 K. The G2(MP2) energies are available as Supporting Information, and the other data data are summarized in Tables2−4.

Table 2. Calculated Methyl Rotational Barriers at the MP2/6-311+G** Level in kcal/mol

	DMTF[b]			DMTA[c]		
methyl group	GS	TS1	TS2	GS	TS1	TS2
C-Me	−	−	−	1.8	2.4	0.9
N-Me(cis)	0.7	3.7	3.1	1.4	3.9	3.4
N-Me(trans)	1.8	3.7	3.1	0.6	3.9	3.4

[a] In the ground state cis and trans refer to the relationship of the methyl to sulfur. [b] In the ground state, the cis methyl C−N−C−H torsional angles are 180° and ±59.8°, and the trans methyl has $\tau = 0°$ and +120.0°. In TS1 the C−N−C−H torsional angles are 173.6°, 55.3°, and −90.6°, whereas in TS2 they are 179.6°, 59.3°, and −61.9°. [c] In the ground state the cis methyl C−N−C−H torsional angles are 180°, and ±59.4°, and the trans methyl has $\tau = 0°$ and ±120.2°. In TS1 they are 158.4°, 54.8°, and −91.0°, whereas in TS2 they are 169.6°, 51.8°, and −70.3°. In all cases, a C-methyl hydrogen is syn to the C═S group.

The G2(MP2) calculated energies include the calculated zero-point energies (ZPE). Since the ZPE values for the above modes will be used instead of the G2(MP2) calculated values, the G2-(MP2) energies without the ZPE are used in the following.

The methyl rotational barriers were calculated at the MP2/6-311+G* level and are given in Table 2.[12] The contribution to the energy change on going from 0 K to 353 K (the temperature used in the NMR experiments) was calculated as described previously.[1] The nitrogen inversion mode was treated as described below.

The thermodynamic corrections are summarized in Table 3, and the final calculated barriers are given in Table 4. With both DMTF and DMTA rotation could proceed via either TS1 or TS2, and the final values are corrected for the participation of the higher-energy transition state. The calculated values are in quite good agreement with the experimental observations.

4. Calculation of the Solvent Effect

The solvent effect was calculated using the SCI-PCM reaction field model at the HF/6-31+G* level allowing for full geometry optimization. The solvation energies are given in Table 5. Since the solvation energies depend only on the structure and the electron density distribution, they are usually not strongly basis set- or model-dependent. This level of theory will give a satisfactory electron density distribution.

To relate the calculated solvent effects to the experimental data for DMTF and DMTA, we have proceeded as follows. The G2/MP2 energy difference, corrected for large amplitude motions described in section 3 was used to estimate the gas-phase energy barriers at 0 K and 353 K (enthalpy and free energy). The changes in solvation free energies calculated at the SCI-PCM level were then included to give the estimates of the barrier heights in solution provided in Table 6. The C−N bond rotation may occur via both TS1 and TS2, and the final calculated barrier heights include the contribution from the two paths.

(12) The methyl rotational barriers for the present compounds as well as for related compounds will be considered in detail in a subsequent report. The MP2/6-311+G** theoretical level has been found to reproduce other rotational barriers: Bohn, R. K.; Wiberg, K. B. *Theor. Chem. Acc.* **1999**, *102*, 272. Wiberg, K. B.; Bohn, R. K.; Jimenez-Vazquez, H. *J. Mol. Struct.* **1999**, *485*, 239.

Table 3. Calculation of Thermodynamic Terms for Thioamides, kcal/mol, 80 °C

	GS				TS1				TS2			
component	$H_0^0 - E$	$H^0 - H_0^0$	S^0	$G^0 - G_0^0$	$H_0^0 - E$	$H^0 - H_0^0$	S^0	$G^0 - G_0^0$	$H_0^0 - E$	$H^0 - H_0^0$	S^0	$G^0 - G_0^0$
a. *N*,*N*-Dimethylthioformamide												
translation	0.00	1.75	40.21	−12.45	0.00	1.75	40.21	−12.45	0.00	1.75	40.21	−12.45
rotation	0.00	1.05	26.91	−8.42	0.00	1.05	26.87	−8.44	0.00	1.05	27.00	−8.48
vibration	59.86	1.82	8.20	−1.08	59.17	1.82	8.09	−1.04	59.11	1.76	7.59	−0.92
N-version	0.18	0.48	2.93	−0.56	0.00	0.00	0.00	0.00	0.00	0.00	0.00	0.00
	0.15	0.48	3.65	−0.81	0.36	0.45	2.23	−0.35	0.36	0.46	2.29	−0.35
Me-rotation[b]	0.24	0.55	3.18	−0.57	0.36	0.45	2.23	−0.35	0.36	0.46	2.29	-0.35
total	60.43	6.13	85.08	−23.89	59.86	5.52	79.63	−22.63	59.83	5.48	79.38	−22.55
b. *N*,*N*-Dimethlthioacetamide												
translation	0.00	1.75	40.65	−12.60	0.00	1.75	40.65	−12.60	0.00	1.75	40.65	−12.60
rotation	0.00	1.05	27.94	−8.81	0.00	1.05	27.91	−8.80	0.00	1.05	27.96	−8.82
vibration	76.51	2.53	11.17	−1.42	75.81	2.51	11.17	−1.43	75.81	2.51	11.05	−1.39
N-inversion	0.17	0.49	3.07	−0.59	0.00	0.00	0.00	0.00	0.00	0.00	0.00	0.00
Me-rotation[b]	0.30	0.53	2.84	−0.47	0.30	0.53	2.84	−0.47	0.15	0.49	3.62	−0.79
Me-rotation[a]	0.21	0.54	3.38	−0.65	0.37	0.46	2.22	−0.34	0.36	0.46	2.31	−0.36
Me-rotation[a]	0.12	0.46	3.68	−0.84	0.37	0.46	2.22	−0.34	0.36	0.46	2.31	−0.36
total	77.31	7.35	92.73	−25.38	76.85	6.76	87.01	−23.98	76.68	6.72	87.90	−24.32

[a] *N*-methyl group. [b] C-methyl group.

Table 4. Calculated Barriers for Thioamide Rotation in kcal/mol ($\Delta S^{\ddagger}$ in cal/mol K)

cmpd	TS	$\Delta H^{\ddagger}$ (0 K)	$\Delta H^{\ddagger}$ (353 K)	$\Delta G^{\ddagger}$ (353 K)	$\Delta S^{\ddagger}$ (353 K)
dimethylthioformamide	1	21.3	20.7	22.6	−5.3
	2	21.2	20.6	22.5	−5.6
	combined			21.9	
dimethylthioacetamide	1	16.9	15.4	17.4	−5.6
	2	19.5	18.9	20.5	−4.8
	combined			17.3	

Table 5. Calculated Solvation Energies, HF/6-31+G*

		relative free energy[a]			
cmpd	conformation	$\epsilon = 2$	$\epsilon = 3$	$\epsilon = 7$	$\epsilon = 80$
N,*N*-dimethylthioformamide	GS	−2.8	−4.1	−5.9	−7.5
	TS1	−0.9	−1.3	−1.9	−2.4
	TS2	−1.4	−2.0	−3.0	−3.8
N,*N*-dimethylthioacetamide	GS	−2.6	−3.9	−5.7	−7.2
	TS1	−1.0	−1.4	−2.1	−2.6
	TS2	−1.5	−2.2	−3.2	−4.2

[a] Energies relative to $\epsilon = 1$, kcal/mol. Dipole moments ($\epsilon = 1$): DMTF, 5.87, 2.09, 3.41. DMTA; 5.83, 2.45, 3.81.

Table 6. Calculated Rotational Barriers in Solution ($\Delta G^{\ddagger}$ (353 K) in kcal/mol)

	DMTF			DMTA		
ϵ	TS1	TS2	combined[a]	TS1	TS2	combined[a]
1	22.6	22.5	21.9	17.4	20.5	17.3
2	24.5	24.0	23.5	19.1	21.7	19.0
3	25.4	24.6	24.2	19.8	22.2	19.8
7	26.6	25.5	25.2	21.0	23.0	20.8
80	27.7	26.2	26.0	21.9	23.5	21.8

[a] Adjusted to take into account the part of the reaction that proceeds via the higher energy transition state.

To compare the calculated and observed solvent effects, the $\Delta G^{\ddagger}$ values have been plotted against the corresponding values of the Onsager function. Figures4 and 5 show plots of the experimental and calculated C−N rotational barriers for DMTA and DMTF. With DMTA, the observed values are uniformly about 0.4 kcal/mol higher than those of the calculated barriers. The small difference arises mainly from the gas-phase calculation. In the case of DMTF the observed values are close to the calculated barriers. In both cases, the agreement between the calculated and observed rotational barriers is satisfactory.

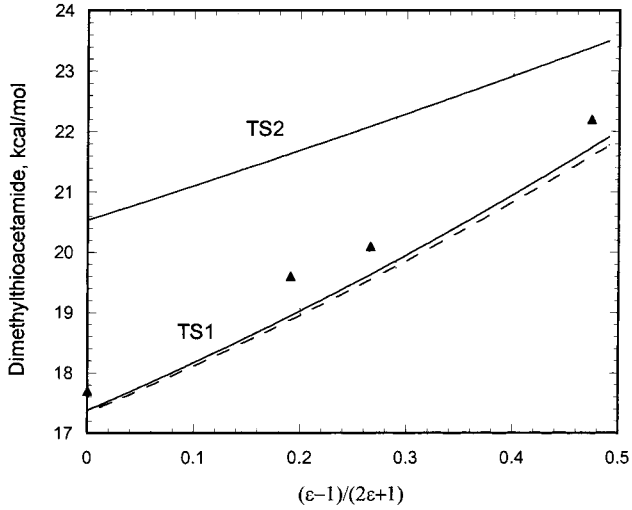

Figure 4. Calculated and observed rotational barriers for DMTA. The lines marked TS1 and TS2 are the calculated barriers, and the dashed line adjacent to the TS1 line is the apparent barrier including both pathways. The solid symbols are the observed barriers in the gas phase, cyclohexane, di-*n*-butyl ether, and acetonitrile.

5. Conclusions

The experimental gas-phase C−N rotational barriers for DMTF and DMTA are well reproduced at the G2(MP2) theoretical level when the large amplitude methyl rotational modes and nitrogen inversion mode are treated separately. The solvent effect on the rotational barrier indicates that DMTF reacts via TS2 and DMTA reacts via TS1. This is the same as previously found for DMF and DMA.

The experimental solvent effects on the rotational barriers are considerably larger for DMTA than for DMA, and this results from the larger ground-state dipole moments for the thioamides than for amides. The dipole moments for the transition state are similar for the two systems. The solvent effects are satisfactorily modeled via the SCI-PCM reaction field model.

6. Origin of the C−N Bond Rotational Barriers

The question of amide "resonance" is closely associated with the C−N bond rotational barriers since rotation will remove the π-interaction between the amide nitrogen and the carbonyl

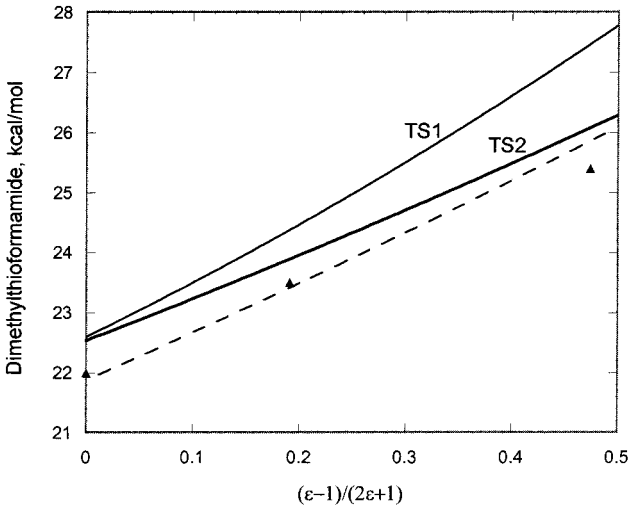

Figure 5. Calculated and observed rotational barriers for DMTF. The lines marked TS1 and TS2 are the calculated barriers, and the dashed line adjacent to the TS2 line is the apparent barrier including both pathways. The closed symbols are the observed barriers in the gas phase, cyclohexane, and acetonitrile.

or C═S group. Some time ago, we pointed out that the traditional resonance formulation:

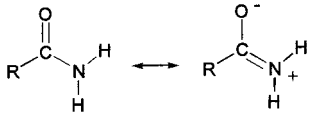

does not appear to be accurate in that the charge transfer to oxygen was found to be small, and whereas the C−N bond underwent a large change in length on rotation, the C═O bond length changed very little.[13] This has led to a large number of related studies.[14] It would seem appropriate at this time to carefully examine what is known and what can be said with certainty.

The experimental observations are as follows:

1. The rotational barrier in amides is fairly large (∼15−20 kcal/mol), and it is increased on going to polar solvents, showing that the ground-state structure is more polar than the transition-state structure.

2. The rotational barrier for thioamides is larger than that for amides, and the solvent effect on the barrier for DMTA is 1.7 times that for DMA. This correlates with the larger dipole moment of DMTA, and its larger change in dipole moment on going to the transition state as compared with DMA.

3. Whereas the C−N bond length increases significantly on rotation from the ground state to the transition state, the C═O bond length decreases by only a small amount.[15] Ab initio calculations found the C═N bond to increase be 0.08 Å, whereas the C−O bond shortened by only 0.01 Å.

4. The carbonyl group is strongly polarized as a result of the difference in electronegativity of carbon and oxygen.

5. The amide group is essentially planar in the ground-state structures, but is markedly pyramidalized in the rotated form.

Additional information derived from ab initio calculations:

1. On rotation from the ground state to the transition state, the carbonyl oxygen of formamide loses 0.07 π electrons and gains 0.03 σ electrons.[4]

2. On rotation from the ground state to the transition state, the thiocarbonyl sulfur of thioformamide loses 0.13 π electrons and gains 0.07 σ electrons.[4]

3. The force constant for the out-of-plane wagging motion of the NH_2 groups is significantly larger for the thioamides than the amides.[4]

With regard to the π-electron changes in the amides, most of these results are readily explained if one writes the following resonance structures:

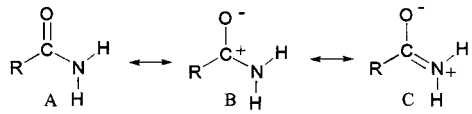

The strong polarization of the C═O group leads to an electron-deficient carbon to which the nitrogen π-electrons may be donated in the ground-state structure. Since the oxygen already bears a large negative charge (derived from both the π and σ systems), there is little to be gained in transferring charge to the oxygen. This can also be stated in FMO[16] terms as follows.[4] The carbonyl π-MO will have the largest coefficient at oxygen because of the difference in electronegativity between carbon and oxygen. Correspondingly, the π^* MO to which the N will donate π-electron density will have the larger coefficient at carbon. Thus, the donation will result in a significant increase in π-density at carbon, and only a small increase at oxygen. In this connection, it might be noted that Glendenning and Hrabal concluded in their recent study that only two resonance structures are needed, but for convenience in calculation, they used structure A to represent *both* the covalent and polar structures (ours are A and B, respectively).[14c] Thus, there is no significant difference between our conclusions and those of Glendenning and Hrabal.

The C═S bond will have only a small polarization since the electronegativities of carbon and sulfur are about the same. Thus, the importance of structure B is markedly reduced. Then, π-donation from N will result in an increase in electron density at both carbon and sulfur. In terms of the FMO model, the C and S coefficients in the π MO will be about the same, and this will also be true for the π^* MO (with opposite signs for the latter). Thus, charge transfer from nitrogen will affect both C and S.[17] The greater charge transfer from N to S in thioamides as compared to from N to O in amides is probably responsible for (a) the greater change in dipole moment on rotation about the C−N bond in thioamides, (b) the stiffer out-of-plane NR_2 vibrational mode of the thioamides, and (c) the larger C−N bond rotational barrier of the thioamides. The increased charge transfer in thioamides also has been found in the calculations of Lauvergnat and Hiberty.[14b]

(13) Wiberg, K. B.; Breneman, C. M. *J. Am. Chem. Soc.* **1992**, *114*, 831. Wiberg, K. B.; Breneman, C. M.; LePage, T. J. *J. Am. Chem. Soc.* **1990**, *112*, 61.

(14) (a) Laidig, K. E.; Cameron, L. M. *J. Am. Chem. Soc.* **1996,** *118*, 1737. (b) Lauvergnat, D.; Hiberty, P. C. *J. Am. Chem. Soc.* **1997**, *119*, 9478. (c) Glendenning, E. D.; Hrabel, J. A., II. *J. Am. Chem. Soc.* **1997**, *119*, 12940. (d) Basch, H.; Hoz, S. *Chem. Phys. Lett.* **1998**, *294*, 117. (e) Hiberty, P. C. *J. Mol. Struct.* **1998**, *451*, 237. (f) Kim. W.; Lee, H. J.; Choi, Y. S.; Choi, J. H.; Yoon, C. J. *J. Chem. Soc., Faraday Trans.* **1998**, *94*, 2663. (g) Raos, G.; Bielli, P.; Tornaghi, E. *Int. J. Quantum. Chem.* **1999**, *74*, 249. (h) Bain, A. D.; Hazendonk, P.; Couture, P. *Can. J. Chem.* **1999**, *77*, 1340. (i) Vassilev, N. G.; Dimitrov, V. S. *J. Mol. Struct.* **2000**, *522*, 37. (j) Breneman, C. M.; Martinov, M. In *The Amide Link*; Greenberg, A., Breneman, C. M., Liebman, J. F., Eds., Wiley: New York, 2000 and earlier references cited within.

(15) Greenberg, A.; Venzanzi, C. A. *J. Am. Chem. Soc.* **1993**, *115*, 6951. Greenberg, A.; Moore, D. T.; Dubois, T. D. *J. Am. Chem. Soc.* **1996**, *118*, 8658.

(16) Fukuii, K. *Acc. Chem. Res.* **1971**, *4*, 57. Fukuii, K.; Fujimoto, H. *Bull. Chem. Soc. Jpn. 1969*, **42**, 3399.

(17) Wiberg, K. B. In *The Amide Link*; Greenberg, A., Breneman, C. M., Liebman, J. F., Ed.; Wiley: New York, 2000; p 41.

The changes in the π-system are only half the story, and this is a problem with most resonance or FMO formulations. In the planar amide, the nitrogen uses sp^2 orbitals to form the bonds (note that the H−N−H bond angle in formamide is 119.1°). However, in the transition state, the nitrogen has reverted to the normal hybridization for amines, in which the lone pair is placed in an orbital with high s-character, and the bonds to nitrogen have high p-character (here the H−N−H bond angle is 105.4°).[13]

As a result of the rehybridization, the nitrogen is more electronegative in the ground state than in the rotational transition state. This will result in a change in the electron populations in the σ bonds, and a shift in the σ-electrons in a direction opposite to the shift in π-electrons. If one studies the amides using Bader's AIM model,[18] one will find that the boundary between C and N is shifted toward the carbon in the planar form (i.e., away from the nitrogen having increased electronegativity). As a result, there is a net shift in total electron density from carbon to nitrogen in the planar form, which results from the larger volume element associated with the planar nitrogen versus the pyramidalized nitrogen. There is nothing "wrong" with this conclusion,[19] except that it ignores the atomic dipoles and higher moments. If one is to reproduce the electrostatic potential about either the planar or rotated amides, one must include the higher moments along with "atomic charges".[20]

On the other hand, if one uses a model such as NPA[21] in which the size of the nitrogen is essentially unchanged on rotation, one will conclude that there is a net shift in total electron density from nitrogen to carbon. It is these problems of interpretation that has led us to directly examine the changes in electron density via the use of density difference maps.[22] One can be confident that the electron density distribution calculated for a molecule using a moderately high theoretical level will be correct.[23] Thus, the difference densities provide a unique approach to examining the changes that occur as a result of bond rotation or other chemical process.

7. Experimental Section

A. Sample Preparation. DMTA was obtained from Frinton Laboratories and was purified by vacuum sublimation. DMTF was obtained from Pfaltz & Bauer and used without further purification. Deuterated solvents were obtained from Aldrich (most cases), Janssen Chimica (toluene), and Cambridge Isotope Laboratories (butyl ether). Carbon tetrachloride and deuterated benzene, toluene, cyclohexane, acetone, acetonitrile, and dichloromethane were treated with 4 Å molecular sieves and BaO prior to use. Deuterated water and methanol were used as received. NMR samples were prepared by placing 1 μL of DMTF or 1 mg of DMTA in 1.0 mL of the appropriate solvent in an NMR tube. The solutions were then subjected to freeze−pump−thaw cycles and vacuum sealed. It was found that imperfections due to vacuum sealing the NMR tubes reduced the maximum temperature attainable before rupture of the tubes. As such, several of the high-temperature thioamide experiments used tubes capped under a nitrogen purge and secured with Teflon tape.

B. Calibration of Variable-Temperature NMR Probe. All NMR experiments were carried out as previously described[1] using a General Electric Ω-300 (300 MHz) spectrometer operated by a Sun workstation and equipped with a variable-temperature 5 mm broadband probe (300/44 5MM 31P-15N/H). The calibration of the probe's temperature controller was established once per week against a vacuum-sealed ethylene glycol standard using the equation below in which $\Delta\delta$ is the chemical shift difference in ppm.[24]

$$T(\mathrm{K}) = 466.5 - 102.0(\Delta\delta)$$

The calibrated temperature at each of eight intervals was calculated as the average of 10 determinations made over a 10 minute period after an hour of temperature equilibration time.

C. Selective Inversion−Recovery Experiments. Selective inversion−recovery (SIR) experiments were then carried out in the standard fashion,[8−9] as previously described.[1] A delay between pulses of 60 s was used to ensure complete relaxation and avoid the artifacts which incomplete relaxation might cause. Tests on DMTF and DMTA revealed no significant effects. At least an hour was allowed for the temperature to equilibrate at a new value before any experiment was carried out.

The integrated peak intensities for a given series of mixing times were then fit to the equation below in a least-squares sense.[25]

$$\ln\left(\frac{(M_0 - M_{za}(t)) - (M_0 - M_{zx}(t))}{(M_0 - M_{za}(t)) + (M_0 - M_{zx}(t))}\right) = -2k_r t$$

M_0 refers to the equilibrium magnetization (intensity), $M_{za}(t)$ the magnetization of peak A at mixing time t, $M_{zx}(t)$ the magnetization of peak X at mixing time t, and k_r the rate constant for exchange. These equations assume equal t_1 relaxation times for the two methyl peaks and make some other assumptions as well. However, as long as exchange is fairly rapid compared to longitudinal relaxation, whether this assumption is correct will make almost no difference for the computed rate constant. An extremely high degree of linearity was obtained, with r^2 values typically 0.995 or better, and almost never below 0.99, although in some cases with slow exchange only two or three half-lives could be used.

In the case of the thioamides, it was found that a baseline correction scheme which was implemented in the script produced improved linearity, particularly at low rates of exchange. At high rates of exchange the corrected and uncorrected values were often not significantly different. The more reliable corrected data were used for the reported barrier data.

The values of $\Delta G^{\ddagger}$ at the listed temperatures were then obtained from the Eyring equation with the transmission coefficient set to 0.5. The results for the thioamides are included as Table 1.

The rates of methyl group exchange in DMF and DMA are known to be concentration dependent in nonpolar solvents, presumably due to association between the molecules.[26] With the benefit of a modern 300 MHz FT spectrometer, we were able to perform all experiments at or near the low concentration limit.

Error Estimates. The error in rate constants determined in these experiments is estimated at ±5%, and the uncertainty in the temperature at ±0.1° (based on the variability of the weekly temperature calibrations), leading to an overall uncertainty of ±0.10 kcal/mol for ΔG.

8. Calculations

The methyl rotational barriers were obtained at the MP2/6-311+G** level by incrementing fixed values of the HCNC or HCCS torsional angles, but allowing the other structural parameters to vary. Inversion potential energy, reduced mass and f_1 kinetic energy terms were calculated at the HF/6-31G* level each 5° of q. For both cases, geometry optimization in all other degrees of freedom was carried out. Substitution of $\mu(q)$

(18) Bader, R. W. F. *Atoms in Molecules: A Quantum Theory*; Clarendon Press: Oxford, 1990.
(19) Perrin, C. L. *J. Am. Chem. Soc*. **1991**, *113*, 2865.
(20) Wiberg, K. B.; Rablen, P. R. *J. Comput. Chem*. **1993**, *14*, 1504.
(21) Reed, A. E.; Weinhold, F.; Curtiss, L. A. *Chem. Rev.* **1988**, *88*, 899.
(22) Wiberg, K. B.; Hadad, C. M.; Rablen, P. R.; Cioslowski, J. *J. Am. Chem. Soc*. **1992,** *114*, 8644. Wiberg, K. B.; Rablen, P. R. *J. Am. Chem. Soc.*, **1993**, *115*, 9234. Wiberg, K. B.; Ochterski, J.; Streitwieser, A *J. Am. Chem. Soc.* **1996**, *118*, 8291.
(23) Volkov, A.; Abramov, Y.; Coppens, P.; Gatti, C *Acta Crystallogr. A* **2000**, *56*, 332.
(24) Ammann, C.; Meier, P.; Merbach, A. E. *J. Magn. Reson.* **1982**, *46*, 319.
(25) Harris, R. K. *Nuclear Magnetic Resonance Spectroscopy*; John Wiley & Sons: New York, 1987; p 172.
(26) Rabinovitz, M.; Pines, A. *J. Chem. Soc. B* **1968**, 1110.

and $f_1(q)$ into the Schrödinger equation was facilitated by modeling each as an eighth order polynomial in even powers. The coefficients were determined by fitting to the data from $q = 0$ to 40° using the Levenberg−Marquardt algorithm[27] and by correcting the reduced mass function to the MP2/6-31G* value at $q = 0°$. Numerical solutions to the Schrödinger equation via the Numerov−Cooley[28] method were converged to better than ± 0.01 cm^{-1} using 2001 points on the inversion coordinate generated by a cubic spline PES interpolation set to keep $\partial^2 V/\partial q^2 = 0$ at the endpoints (natural spline). The resulting energy levels were scaled by 0.8934, the usual factor for frequencies calculated at the HF/6-31G* level.[29]

The ab initio calculations were carried out using Gaussian-95.[30]

Acknowledgment. This investigation was supported by a grant from the National Institute of Health. We thank Professor Robert Champion for his assistance with the variable reduced mass adaptation of the Numerov−Cooley integration method and Dr. Bruce R. Johnson for providing a copy of his program for calculating vibrational energy levels using the above method.

Appendix. Thermodynamic Corrections for Methyl Rotors and Nitrogen Inversion

General. The partition function for a molecule must be calculated to compute thermodynamic quantities such as enthalpy, entropy, and free energy at temperatures above absolute zero from ab initio calculations. The partition function is generally separated into translational, rotational, and vibrational components. The first two can be treated in the usual fashion[31] If the vibrational modes are approximately harmonic, they may be treated in the corresponding fashion.

However, if one or more modes are not well described by a harmonic oscillator potential function, a more appropriate approximation is required. Usually the low-frequency modes are the ones least well represented by a harmonic oscillator. Thus, the effects on the zero-point energy and the enthalpy are generally small, but the effects on the entropy, and thus the free energy, can be substantial. In DMTF and DMTA, the methyl rotors and the nitrogen inversion mode are the most important cases in which the harmonic oscillator approximation is poor. These modes were treated separately.

Methyl Rotors. The method used for determining the partition function for the methyl rotors has been previously described.[1] The calculated rotational barriers are given in Table 3.

Nitrogen Inversion. The inversion vibrational modes derived from the frequency calculation for DMTF were readily located using Gaussview.[32] The assignment of the inversion vibrational frequencies for the ground state of DMTA was difficult in that there are significant contributions from modes at 310 and 595 cm^{-1}. The choice of which frequency to replace changed the barrier from 17.6 (595 cm^{-1}) to 17.1 (310 cm^{-1}) kcal/mol. In the end, we used the average contribution from the modes, arriving at the final calculated barrier of 17.3 kcal/mol.

Introduction. As insufficient experimental data exist to obtain the literature values for many nitrogen inversion energy levels, a reasonable alternative is to calculate these properties ab initio. With this in mind, we developed a method, successfully tested it on the ν_2 nitrogen inversion mode of ammonia,[33] and have now applied it to thioamide systems. This method shows more basis set consistency for the vibrational transitions and thermodynamic properties when compared to use of the harmonic oscillator vibrational frequencies. Calculated free energy contributions of the inversion mode for formamide and acetamide at the HF/6-31G* and MP2/6-31+g** levels are within 5% of those estimated from experimental data.[34] High-level calculations on ammonia resulted in good agreement with the experimental inversion energy levels,[35] and calculations on DMF and DMA C−N rotational barriers were in good agreement with experiment.[1,3]Energy levels for the thioamide nitrogen inversion mode are solutions to the one-dimensional, time-independent Schrödinger equation below.[36]

$$-\frac{h^2 \mathrm{d}^2\psi(q)}{2\mu\ \mathrm{d}q^2} + [V(q) - E]\psi(q) = 0$$

Here q is the inversion coordinate, μ is the reduced mass appropriate for q, and $V(q)$ is the inversion potential function. Ab initio theory has been used to construct and solve this equation for DMTF and DMTA.

Inversion Coordinate. To define the inversion coordinate, a *Z*-matrix was constructed which forced an imaginary atom to maintain equal angles between itself, nitrogen, and the three nitrogen substituents. We chose to describe the inversion coordinate q as the amount of pyramidalization occurring at the nitrogen atom, where the value of q is the X−N−R angle minus 90°. It allows a full range of motion for the nitrogen substituents, while permitting easy calculation of the ab initio potential function for any value of q. These calculations included full geometry optimization for all other degrees of freedom that allowed for some coupling between the inversion motion and other modes through both the potential function and the reduced mass.

Potential Function. The ab initio inversion potential function was also calculated with full geometry optimization in all other modes. After discovering some problems modeling the ammonia PES with polynomial functions, we elected to model the thioamide PES using a spline interpolation of points.

Reduced Mass. We decided to calculate the reduced mass using a numerical method adapted from the work of Laane and co-workers.[37] With the atomic positions known as a function of the coordinate from optimized ab initio geometries, the vibrational−rotational **G** matrix may be determined using equations taken from Laane.[38]

(27) Marquardt, D. W. *J. Soc. Ind. Appl. Math*, **1963**, *11*, 431.
(28) Cooley, J. W. *Math. Comput.* **1961**, *15*, 363.
(29) Pople, J. A.; Head-Gordon, M.; Fox, D. J.; Raghavachari, K.; Curtiss, L. A. *J. Chem. Phys.* **1989**, *90*, 5622.
(30) Frisch, M. J.; Trucks; G. W.; Schlegel, H. B.; Gill, P. M. W.; Johnson, B. G.; Robb; M. A.; Cheeseman, J. R.; Keith, T.; Petersson, G. A.; Montgomery, J. A.; Raghavachari, K.; Al-Laham, M. A.; Zakrzewski, V. G.; Ortis, J. V.; Foresman, J. B.; Cioslowski, J.; Sefanov, B. B.; Nanayakkara, A.; Challacombe, M.; Peng, C. Y.; Ayala, P. Y.; Chen, W.; Wong, M. W.; Andres, J. L.; Replogle, E. S.; Gomperts, R.; Martin, R. L.; Fox, D. J.; Binkley, J. S.; Defrees, D. J.; Baker, J.; Stewart, J. P.; Head-Gordon, M.; Gonzalez, C.; Pople, J. A. *Gaussian 95*; Development Version (rev. D) Gaussian, Inc.: Pittsburgh, PA, 1995.
(31) Janz, G. J. *Thermodynamic Properties of Organic Compounds: Estimation Methods, Principles and Practice*, revised ed.; Academic Press: New York, 1967.
(32) Gaussview 2.0, Gaussian, Inc.: Pittsburgh, PA.
(33) Rush, D. J.; Wiberg, K. B. *J. Phys. Chem.* **1997**, *101*, 3143.
(34) Hansen, E. L.; Larsen, N. W.; Nicolaisen, F. M. *Chem. Phys. Lett.* **1980**, *69*, 327.
(35) Spirko, V. *J. Mol. Spectrosc.* **1983**, *101*, 30.
(36) Atkins, P. W. *Molecular Quantum Mechanics*, 2nd ed.; Oxford University Press: New York, 1983.
(37) Laane, J.; Harthcock, M. A.; Killough, P. M.; Bauman, L. E.; Cooke, J. M. *J. Mol. Spectrosc.* **1982**, *91*, 286.
(38) Laane, J.; Harthcock, M. A. *J. Mol. Spectrosc.* **1982**, *91*, 300.

$$\mathbf{G} = \begin{bmatrix} \mathbf{I} & \mathbf{X} \\ \mathrm{X}^{\mathrm{t}} & \mathbf{Y} \end{bmatrix}^{-1}$$

Here, **I** is the 3 × 3 rotational moment of inertia tensor, **X** is a 3x(3N-6) matrix containing information on vibrational−rotational coupling, and **Y** is a (3N-6)x(3N-6) matrix representing the vibrational contribution. Looking at the inversion vibration alone assumes decoupling from all other vibrational modes and produces the 4 × 4 matrix below designated **G**(q).

$$\mathbf{G}(q) = \begin{bmatrix} \mathbf{I}_{xx} & -\mathbf{I}_{xy} & -\mathrm{I}_{xz} & \mathrm{X}_{11} \\ -\mathrm{I}_{xy} & \mathrm{I}_{yy} & -\mathrm{I}_{yz} & \mathrm{X}_{21} \\ -\mathrm{I}_{xz} & -\mathrm{I}_{yz} & \mathrm{I}_{zz} & \mathrm{X}_{31} \\ \mathrm{X}_{11} & \mathrm{X}_{21} & \mathrm{X}_{31} & \mathbf{Y}_{11} \end{bmatrix}^{-1}$$

The matrix elements are defined below where i are the x, y, or z fixed molecular axes, N is the total number of atoms, m_α is the mass of atom α, $\mathbf{r}_\alpha$ is the position vector of atom α relative to the center of mass, and $\mathbf{r}_{\alpha i}$ and $\mathbf{r}_{\alpha k}$ are the ith and kth components of the αth vector.

$$\mathbf{I}_{ii} = \sum_{\alpha=1}^{N} m_\alpha (\mathbf{r}_\alpha \cdot \mathbf{r}_\alpha - \mathbf{r}_{\alpha i}^2)$$

$$\mathbf{I}_{ik} = \sum_{\alpha=1}^{N} m_\alpha \boldsymbol{r}_{\alpha i} \boldsymbol{r}_{\alpha k}, \quad i \neq k$$

$$\mathbf{X}_{ik} = \sum_{\alpha=1}^{N} m_\alpha \left[\mathbf{r}_\alpha \times \left(\frac{\partial \mathbf{r}_\alpha}{\partial q_k} \right) \right]_i$$

$$\mathbf{Y}_{ik} = \sum_{\alpha=1}^{N} m_\alpha \left(\frac{\partial \mathbf{r}_\alpha}{\partial q_i} \right) \cdot \left(\frac{\partial \mathbf{r}_\alpha}{\partial \boldsymbol{q}_k} \right)$$

The matrix can be inverted using standard computer subroutines to obtain the form below.[39]

$$\mathbf{G}(q) = \begin{bmatrix} g_{11} & g_{12} & g_{13} & g_{14} \\ g_{21} & g_{22} & g_{23} & g_{24} \\ g_{31} & g_{32} & g_{33} & g_{34} \\ g_{41} & g_{42} & g_{43} & g_{44} \end{bmatrix}$$

For a given position along the coordinate of our single inversion vibration, the reduced mass is determined from the g_{44} term.

$$g_{44} = \frac{1}{\mu}$$

The **G**(q) matrix was calculated at many positions along the inversion coordinate to enable the calculation of the reduced mass as a function of q.

This method was implemented by a series of FORTRAN programs that were written to utilize the output from our electronic structure calculations. The atomic positions in Cartesian coordinates were translated to a center of mass reference and the molecule rotated into the principal axis system. Elements for the **G**(q) matrix were calculated using the previously mentioned formulas. The partial derivatives were approximated by taking differences in atomic position for 0.1° changes in coordinate q. The reduced mass was mapped as a function of inversion coordinate q, then fit to an eighth order polynomial in even powers for insertion into the Schrödinger equation.

Schrödinger Equation. There are some complications introduced into the mathematics of the Schrödinger equation when the reduced mass is included as a function of coordinate. Hougen, Bunker, and Johns (HBJ), in their paper describing the "rigid bender" derivation for triatomics,[40] build upon work summarized by Wilson, Decius, and Cross[41] to solve this problem. By looking simply at the large amplitude motion (LAM) vibrational energy levels and assuming the rotational energies in their ground states with quantum numbers, $J_x = J_y = J_z = 0$, HBJ derive the zeroth-order rotational-LAM Hamiltonian below.

$$H_{\mathrm{b}}^0 = -\frac{h^2}{2\mu(q)}\frac{\partial^2}{\partial q^2} - \frac{h^2}{2}\left(\frac{\partial}{\partial q}\frac{1}{\mu(q)}\right)\frac{\partial}{\partial q} - \frac{h^2}{2}|\mathbf{G}(q)|^{-1/4}\left\{\frac{\partial}{\partial q}\frac{1}{\mu(q)}\left|\mathbf{G}(q)\right|^{1/2}\left[\frac{\partial}{\partial q}\left|\mathbf{G}(q)\right|^{1/4}\right]\right\} + V(q) \quad (1)$$

Here $|\mathbf{G}(q)|$ is the determinant of the **G**(q) matrix, and $\mu(q)$ is the reduced mass as a function of the inversion coordinate q. This equation has been simplified by fixing all normal coordinates at their equilibrium values and ignoring the vibrational angular momenta. This effectively holds the small amplitude motions at their equilibrium values while the LAM occurs.

The linear derivative term in eq 1 may be removed using the substitution

$$\psi_{\mathrm{b}}(q) = \mu(q)^{1/2}\phi_{\mathrm{b}}(q) \quad (2)$$

which has the effect of changing the volume element from dq to $\mu(q)$dq. This provides a Schrödinger equation of the form

$$\frac{\partial^2}{\partial q^2}\phi_b(q) = \left\{f_1(q) + \frac{2\mu(q)}{\hbar^2}[V_0(q) - E]\right\}\phi_b(q) \quad (3)$$

$$f_1(q) = |\mathbf{G}(q)|^{1/4}\mu(q)^{1/2}\left\{\frac{\partial^2}{\partial q^2}[|\mathbf{G}(q)|^{-1/4}\mu(q)^{-1/2}]\right\} \quad (4)$$

where the $f_1(q)$ term is nearly constant for systems of greater than three atoms.[42] The Schrödinger equation has thus been reduced to its familiar form for a one-dimensional potential, which now includes the reduced mass as a function of LAM coordinate. The wave function ϕ_b must be transformed by eq 2 to give the original wave function Ψ_{b} appropriate for the energy level in question.

Numerov−Cooley Method. Solutions to the one-dimensional Schrödinger eq 3 were obtained for the vibrational energy levels using the Numerov−Cooley[26,43] algorithm implemented in a FORTRAN program.[44] This numerical method was developed to solve second-order differential equations of the form

$$\left[\frac{\mathrm{d}^2}{\mathrm{d}q^2} + Q(q)\right]\psi(q) = 0 \quad (5)$$

(39) Press: W. H.; Flannery, B. P.; Teukolsky, S. A.; Vetterling, W. T. *Numerical Recipes: The Art of Scientific Computing; FORTRAN Version;* Cambridge University Press: New York, 1990.

(40) Hougen, J. T.; Bunker, P. R.; Johns, J. W. C. *J. Mol. Spectrosc.* **1970**, *34*, 136.

(41) Wilson, E. B., Jr.; Decius, J, C.; Cross, P. C. *Molecular Vibrations: The Theory of Infrared and Raman Vibrational Spectra*; McGraw-Hill: New York, 1955.

(42) Professor Robert Champion, private communication.

(43) Johnson, B. R. *J. Chem. Phys.* **1977**, *67*, 4086.

(44) Algorithm subroutines written by Dr. Bruce R. Johnson, Rice Quantum Institute.

By setting $Q(q) = (2\mu)/(h^2)[E - V(q)$ this allows us to solve the Schrödinger equation.

Our implementation utilizes the renormalized Numerov method of Johnson.[45] Combining this algorithm with the work of HBJ, FORTRAN subroutines containing this code were modified to accept the reduced mass as a function of coordinate and transform the wave function back into its original form via eq 2.

Supporting Information Available: Tables of G2(MP2) energies of thioamides and of the MP2/6-31G* structures used in the G2(MP2) calculations (PDF). This material is available free of charge via the Internet at http://pubs.acs.org.

JA003586Y

(45) Johnson, B. R. *J. Chem. Phys.* **1978**, *69*, 4678.